RESEARCH ACTIVITIES
Life and Coordination-Complex Molecular Science

Department of Life and Coordination-Complex Molecular Science is composed of two divisions of biomolecular science, two divisions of coordination-complex molecular science, and one adjunct division. Biomolecular science divisions cover the studies on functions, dynamic structures, and mechanisms for various biomolecules such as sensor proteins, membrane-anchored proteins, biological-clock proteins, metalloproteins, glycoconjugates, and molecular chaperone. Coordination complex divisions aim to develop molecular catalysts and functional metal complexes for transformation of organic molecules, water oxidation and reduction, and molecular materials such as molecular wires. Interdisciplinary alliances in this department aim to create new basic concepts for the molecular and energy conversion through the fundamental science conducted at each division. Professor Koji Tanaka was retired at the end of March, 2012. Professors Shuji Akiyama and Tetsuro Murahashi were appointed as full professors of the Division of Biomolecular Sensing and the Division of Functional Coordination Chemistry, respectively, both in April, 2012.

Bioinorganic Chemistry of Metal-Containing Sensor Proteins

**Department of Life and Coordination-Complex Molecular Science
Division of Biomolecular Functions**

AONO, Shigetoshi   Professor
YOSHIOKA, Shiro   Assistant Professor
SAWAI, Hitomi   IMS Research Assistant Professor
TANIZAWA, Misako   Secretary

The widely studied biological function of heme is to act as a prosthetic group in hemeproteins that show a variety of functions, including oxygen storage and transport, electron transfer, redox catalysis, and sensing of gas molecules. In addition to these functions, a new function of hemeprotein has been found recently, which is a sensor of diatomic gas molecules or redox change.[1] In these heme-based sensor proteins, the heme acts as the active site for sensing the external signal such as gas molecules and redox change. A new hemeprotein, aldoxime dehydratase (Oxd), also shows a novel biological function of heme, which catalyzes dehydration reaction of organic substrates. Oxd is the first example of hemeproteins that act as a hydro-lyase. Our research interests are focused on the elucidation of the structure-function relationships of these hemeproteins.

1. Bacterial Gas Sensor Proteins Using Transition Metal-Containing Prosthetic Groups as Active Sites[2,3]

Gas sensor proteins are involved in many biological regulatory systems, including transcription, chemotaxis, and other complex physiological processes. These regulatory systems consist of a sensor and regulatory protein, and, if any, signal transduction proteins that transmit the input signal sensed by the sensor protein to regulator proteins. Sensor proteins are the most upstream component in these regulatory systems, and the sensor and regulator proteins can be distinct molecules, or can sometimes exist in the same molecule as sensor and regulator domains. In both cases, the general scheme is as follows for biological regulatory systems by gas sensor proteins. Once a gas sensor protein/domain senses a gas molecule of its physiological effector, a conformational change of the sensor protein/ domain is induced, and then intra- and/or inter-molecular signal transductions proceed to modulate the activity of the regulator protein/domain that is responsible for the regulation of the above biological functions.

HemAT from *Bacillus subtilis* (HemAT-*Bs*) is a heme-containing O_2 sensor protein that acts as a chemotactic signal transducer. Binding of O_2 to the heme in the sensor domain of HemAT-*Bs* induces a conformational change in the protein matrix, and this is transmitted to a signaling domain. To characterize the specific mechanism of O_2-dependent conformational changes in HemAT-*Bs*, we investigated time-resolved resonance Raman spectra of the truncated sensor domain and the full-length HemAT-*Bs* upon O_2 and CO dissociation.

A comparison between the O_2 and CO complexes provides insights on O_2/CO discrimination in HemAT-*Bs*. While no spectral changes upon CO dissociation were observed in our experimental time window between 10 ns and 100 μs, the band position of the stretching mode between the heme iron and the proximal histidine, ν(Fe–His), for the O_2-dissociated HemAT-*Bs* was lower than that for the deoxy form on time-resolved resonance Raman spectra. This spectral change specific to O_2 dissociation would be associated with the O_2/CO discrimination in HemAT-*Bs*. We also compared the results obtained for the truncated sensor domain and the full-length HemAT-*Bs*, which showed that the structural dynamics related to O_2 dissociation for the full-length HemAT-*Bs* are faster than those for the sensor domain HemAT-*Bs*. This indicates that the heme proximal structural dynamics upon O_2 dissociation are coupled with signal transduction in HemAT-*Bs*.

We have also studied the protein dynamics of HemAT-*Bs* following CO photodissociation by time-resolved ultraviolet resonance Raman spectroscopy (UVRR). The UVRR spectra indicated two phases of intensity changes for Trp, Tyr, and Phe bands of both full-length and sensor domain proteins. The

W16 and W3 Raman bands of Trp, the F8a band of Phe, and the Y8a band of Tyr increased in intensity at hundreds of nanoseconds after CO photodissociation, and this was followed by recovery in ~50 μs. These changes were assigned to Trp-132 (G-helix), Tyr-70 (B-helix), and Phe-69 (B-helix) and/or Phe-137 (G-helix), suggesting that the change in the heme structure drives the displacement of B- and G-helices. The UVRR difference spectra of the sensor domain displayed a positive peak for amide I in hundreds of nanoseconds after photolysis, which was followed by recovery in ~50 μs. This difference band was absent in the spectra of the full-length protein, suggesting that the isolated sensor domain undergoes conformational changes of the protein backbone upon CO photolysis and that the changes are restrained by the signaling domain. The time-resolved difference spectrum at 200 μs exhibited a pattern similar to that of the static (reduced–CO) difference spectrum, although the peak intensities were much weaker. Thus, the rearrangements of the protein moiety toward the equilibrium ligand-free structure occur in a time range of hundreds of microseconds.
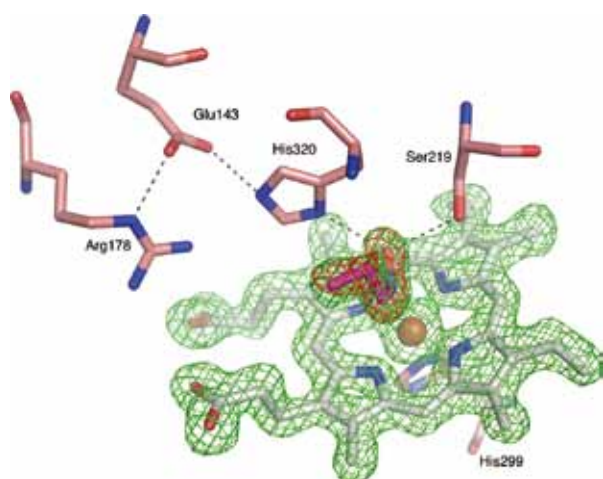
2. Spectroscopic Analyses of the Heme Environmental Structure of Aldoxime Dehydratase[4)]

Aldoxime dehydratase (Oxd) is a new heme-containing enzyme that works as a hydro-lyase catalyzing dehydration of aldoximes to nitriles. The enzymatic activity of Oxd is dependent on the oxidation state of the heme iron, though the reaction catalyzed by Oxd is not a redox reaction. Ferrous Oxd containing a Fe^{2+}-heme shows the enzymatic activity, but ferric Oxd containing a Fe^{3+}-heme does not. Previous spectroscopic analyses reveal a novel mechanism, where the change in the

Figure 1. Heme environmental structure of the substrate-bound OxdRE.

coordination mode of the substrate plays a crucial role for the regulation of the enzymatic activity. Unlike other heme enzymes, the organic substrate is directly bound to the heme iron in OxdRE. While the oxygen atom of aldoxime is coordinated to the ferric heme, the nitrogen atom of aldoxime is coordinated to the ferrous heme. The dehydration reaction proceeds only via N-coordinated substrate in the ferrous heme.

In this study, we have elucidated the heme environmental structure of Oxd from *Rhodococcus sp.* N-771 (OxdRE) by analyzing Fourier transform infrared (FTIR) spectra and time-resolved step-scan FTIR spectra of CO-bound Oxd. Two C–O modes of heme at 1945 and 1964 cm^{-1} have been identified and remained unchanged in H_2O/D_2O exchange and in the pH 5.6–8.5 range, suggesting the presence of two conformations at the active site. The "light" minus "dark" difference FTIR spectra indicate that the heme propionates are in both the protonated and deprotonated forms, and the photolyzed CO becomes trapped within a ligand docking site (ν(CO) = 2138 cm^{-1}). The time-resolved step-scan FTIR spectra show that the rate of recombination of CO to the heme is $k_{1945\ cm^{-1}} = 126 \pm 20\ s^{-1}$ and $k_{1964\ cm^{-1}} = 122 \pm 20\ s^{-1}$ at pH 5.6, and $k_{1945\ cm^{-1}} = 148 \pm 30\ s^{-1}$ and $k_{1964\ cm^{-1}} = 158 \pm 32\ s^{-1}$ at pH 8.5. The rate of decay of the heme propionate vibrations is on a time scale coincident with the rate of rebinding, suggesting that there is a coupling between ligation dynamics in the distal heme environment and the environment sensed by the heme propionates.

The vibrational properties of the CO adduct of OxdRE indicate the formation of a photolabile species in which the proximal histidine and the H-bonding interactions of the negatively charged heme propionates are dominant factors in controlling the strength of the Fe–CO bond. The latter observation indicates that other factors beyond the well-known proximal and distal back-bonding contributions are effective in Oxd. Taken together, these results indicate that the distal residues control the proper orientation of the bound aldoxime and, thus, modulate the heme conformation from inactive to active. Obviously, there is communication linkage between the distal and proximal sites through bond networks suggesting that there is a coupling between ligation dynamics and the environment sensed by the heme propionates. The complexity of the structural implications involved in the transition from oxidized to reduced state in the presence of aldoxime should serve as a basis for uncovering the dynamic processes involved in the reaction mechanism of the enzyme.

References

1) S. Aono, *Dalton Trans.* 3125–3248 (2008).

2) S. El-Mashtoly *et. al.*, *J. Biol. Chem.* **287**, 19973–19984 (2012).

3) Y. Yoshida *et. al.*, *Biochim. Biophys. Acta, Proteins Proteomics* **1824**, 866–872 (2012).

4) E. Pinakoulaki *et. al.*, *J. Phys. Chem. B* **115**, 13012–13018 (2011).

Elucidation of the Molecular Mechanisms of Protein Folding

Department of Life and Coordination-Complex Molecular Science
Division of Biomolecular Functions
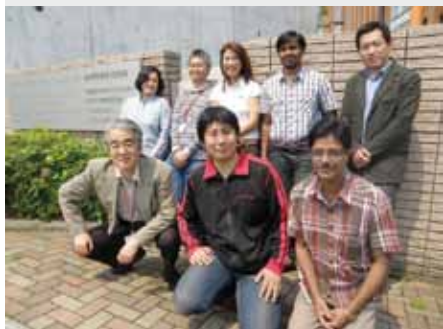
KUWAJIMA, Kunihiro	Professor
MAKABE, Koki	Assistant Professor
NAKAMURA, Takashi	IMS Research Assistant Professor
CHEN, Jin	OIIB Research Assistant Professor
TAKENAKA, Toshio	Post-Doctoral Fellow
MIZUKI, Hiroko	Technical Fellow
TANAKA, Kei	Secretary

Kuwajima group is studying mechanisms of *in vitro* protein folding and mechanisms of molecular chaperone function. Our goals are to elucidate the physical principles by which a protein organizes its specific native structure from the amino acid sequence. In this year, we studied the fibrillogenic propensity of the GrEL apical domain and the sequential four-state folding/unfolding of goat α-lactalbumin and its N-terminal variants.

1. Fibrillogenic Propensity of the GroEL Apical Domain: A Janus-Faced Minichaperone

The chaperonin GroEL plays an essential role in promoting protein folding and in protecting against misfolding and aggregation in the cellular environment. In this study, we report that both GroEL and its isolated apical domain form amyloid-like fibrils under physiological conditions, and that the fibrillation of the apical domain is accelerated under acidic conditions. We also found, however, that despite its fibrillation propensity, the apical domain exhibits a pronounced inhibitory effect on the fibril growth of β_2-microglobulin. The analysis of the primary amino-acid sequence by programs, PASTA, TANGO and Zyggregator, which predict aggregation-prone sequences, indicates that the most aggregation-prone sequence is located in residues 260–280, which is coincident with the substrate protein-binding site in the chaperonin GroEL. Therefore, there is a close relationship between the fibrillogenic propensity and the substrate binding of GroEL. Furthermore, the analysis of 1003 sequences of the chaperonin family proteins by the Zyggregator program has shown that the aggregation-prone sequence is present in the substrate-binding site, indicating that the close relationship between the fibrillogenic propensity and the substrate binding is a general property of the chaperonin family.
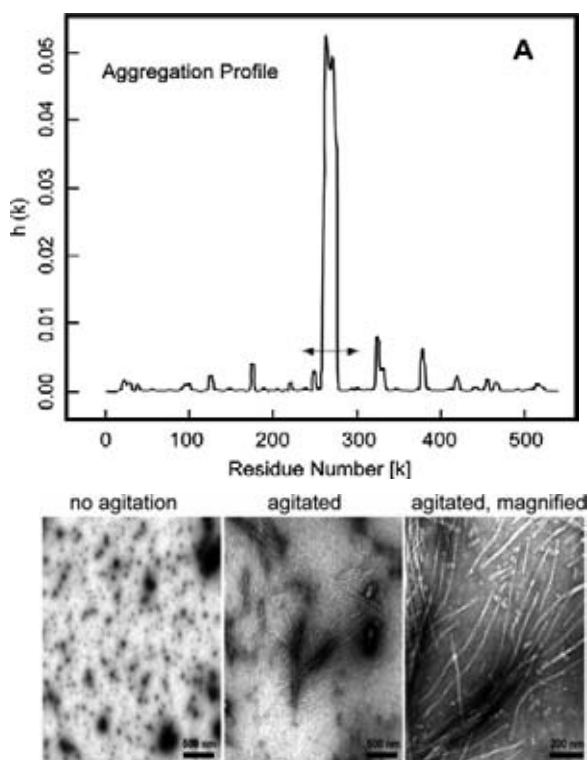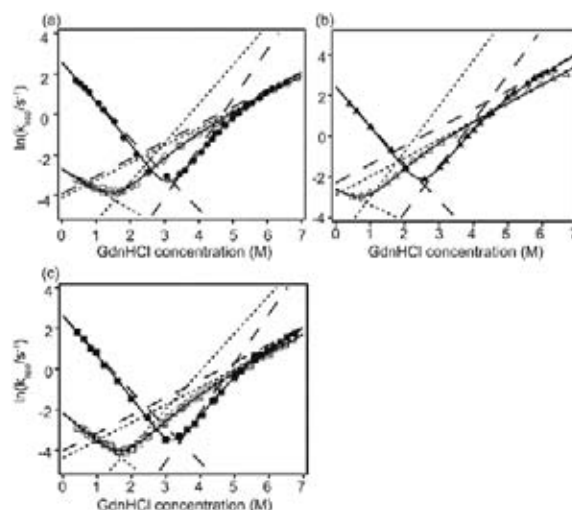

Figure 1. The aggregation profile of GroEL obtained by the analysis with PASTA (A), and the transmission electron microscopic observations of the isolated apical domain at pH 7.0 and 37 °C at 0.1 M NaCl in the presence of 0.5 mM SDS, where the amyloid-like fibrils of the apical domain were formed when the solution was agitated.

## 2. Sequential Four-State Folding/Unfolding of Goat α-Lactalbumin and Its N-Terminal Variants

Equilibria and kinetics of folding/unfolding of goat α-lactalbumin (GLA) and its two N-terminal variants were studied by circular dichroism spectroscopy. The two variants were wild-type recombinant and Glu1-deletion (E1M) variants expressed in *Escherichia coli*. The presence of an extra methionine at the N terminus in recombinant GLA destabilized the protein by 2 kcal/mol, while the stability was recovered in the E1M variant in which Glu1 was replaced by Met1. Kinetic folding/unfolding reactions of the proteins, induced by stopped-flow concentration jumps of guanidine hydrochloride, indicated the presence of a burst-phase in refolding, and gave chevron plots with significant curvatures in both the folding and unfolding limbs. The folding-limb curvature was interpreted in terms of accumulation of the burst-phase intermediate (I). However, there was no burst phase observed in the unfolding kinetics to interpret the unfolding-limb curvature. We thus assumed a sequential four-state mechanism, in which the folding from the burst-phase intermediate takes place via two transition states separated by a high-energy intermediate (J). We estimated changes in the free energies of the burst-phase intermediate I and two transition states (‡1 and ‡2), caused by the N-terminal variations and also by the presence of stabilizing calcium ions. The Φ values at the N terminus and at the Ca^{2+}-binding site thus obtained increased successively during folding, demonstrating the validity of the sequential mechanism. The stability and the folding behavior of the E1M variant were essentially identical to those of the authentic protein, allowing us to use this variant as a pseudo-wild-type GLA in future studies.

Figure 3. Chevron plots of authentic GLA (a), recombinant GLA (b), and the E1M variant (c) in the holo (filled symbols) and apo (open symbols) forms at pH 7.0 and 25 °C. The solid lines are theoretical curves fitted by the sequential four-state model. The broken lines and dotted lines represent the GdnHCl dependence of logarithms of microscopic rate constants ($\ln(k_1)$, $\ln(k_{-1}k_2/k_2)$ and $\ln(k_{-2})$) of folding and unfolding kinetics; the first two are rate-limited by the transition state 1 (‡1), and the last one by the transitions state 2 (‡2).

| Residue No. | 0 | 1 | 2 | 3 | 4 | 5 | 6 | 7 | 8 | 9 | 10 |
Protein											
Authentic GLA		E	Q	L	T	K	C	E	V	F	Q
Recombinant GLA	M	E	Q	L	T	K	C	E	V	F	Q
E1M variant		M	Q	L	T	K	C	E	V	F	Q

Figure 2. The amino acid sequences of the N-terminal residues of authentic GLA, recombinant GLA, and the E1M variant.
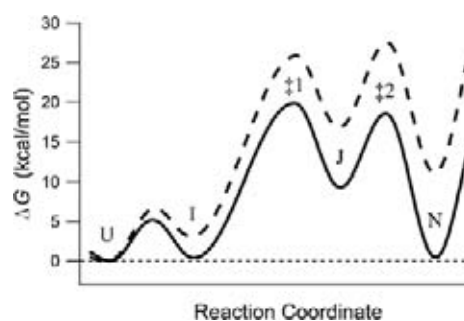
Figure 4. Schematic free-energy profiles of unfolding of GLA under a weakly unfolding condition (solid line) and under a strongly unfolding condition (broken line). Under the weakly unfolding condition, the transition state is located at ‡1, while it is located at ‡2 under the strongly unfolding condition at a high GdnHCl concentration (>5.5*M*). The free-energy profiles shown correspond to those for authentic holo GLA at 3.3*M* GdnHCl (solid line) and at 6.5*M* GdnHCl (broken line). A hypothetical intermediate (J) located between ‡1 and ‡2 is metastable under all conditions, that is, it is higher in free energy than U, I, and N.

References

1) J. Chen, H. Yagi, P. Sormanni, M. Vendruscolo, K. Makabe, T. Nakamura, Y. Goto and K. Kuwajima, *FEBS Lett.* **586**, 1120–1127 (2012).

2) K. Tomoyori, T. Nakamura, K. Makabe, K. Maki, K. Saeki and K. Kuwajima, *Proteins; Struct., Funct., Bioinf.* **80**, 2191–2206 (2012).

Elucidation of Dynamical Structures of Biomolecules toward Understanding the Mechanisms Underlying Their Functions

Department of Life and Coordination-Complex Molecular Science
Division of Biomolecular Functions

KATO, Koichi	Professor
YAMAGUCHI, Takumi	Assistant Professor
KAMIYA, Yukiko	IMS Research Assistant Professor*
YAGI-UTSUMI, Maho	OIIB Research Assistant Professor
YANAGI, Kotaro	IMS Fellow
UEKUSA, Yoshinori	Post-Doctoral Fellow
BOONSRI, Pornthip	Visiting Scientist
BUI DINH, Long	Visiting Scientist
SUGIHARA, Takahiro	Research Fellow
CHANDAK, Mahesh	Graduate Student
ZHANG, Ying	Graduate Student
KUNIHARA, Tomoko	Graduate Student
UNO, Tsuyoshi	Graduate Student†
YAMAMOTO, Sayoko	Graduate Student†
KUMOI, Kentaro	Graduate Student†
OKAWA, Keisuke	Graduate Student†
INAGAKI, Kouya	Graduate Student†
THAMMAPORN, Ratsupa	Graduate Student‡
SUZUKI, Mariko	Technical Fellow
ISONO, Yukiko	Technical Fellow
TANAKA, Kei	Secretary

Our biomolecular studies are based on detailed analyses of structures and dynamics of various biological macromolecules and their complexes at atomic level, using NMR spectroscopy and X-ray crystallography in conjunction with other biophysical, biochemical and molecular biology techniques. Here we report our recent studies of conformations, dynamics, and interactions of oligosaccharides and glycoconjugates along with proteins involved in the ubiquitin (Ub)-proteasome system.

1. Lanthanide-Assisted NMR Analyses of the Conformational Ensemble of Oligosaccharides in Conjunction with Molecular Dynamics Simulations

Conformational flexibility is an important property of biological molecules functioning in living systems, as best exemplified by oligosaccharides. We attempted to combine the lanthanide-assisted NMR method with molecular dynamics (MD) simulations for the evaluation of dynamic conformational ensembles of highly flexible oligosaccharides. In this approach, a metal-chelating tag was covalently attached to the reducing end of the oligosaccharide moieties of gangliosides, which form integral parts of cellular membranes, for observing pseudocontact shifts (PCSs). Upon complexation with paramagnetic lanthanide ions, the tagged GM3 trisaccharide, which is the common core structure shared among the gangliosides, exhibited NMR spectral changes due to PCSs according to the relative positions of the individual atoms with

respect to the lanthanide ion coordinated at the tag. The observed PCS values were in excellent agreement with those back-calculated from the vast conformational ensemble of the trisaccharide derived from MD simulations (Figure 1). Thus, the PCS measurements offer a valuable experimental tool for the validation of MD simulation of highly flexible biomolecules.[1] Furthermore, this approach was successfully applied to the characterization of the conformational dynamics of the branched tetrasaccharide of ganglioside GM2.[2] The interbranch interactions responsible for the conformational differences between the GM2 tetrasaccharide and the GM3 trisaccharide were identified by the paramagnetic NMR method in conjunction with MD simulations. These results demonstrated the utility of our approach in the evaluation of dynamic conformational ensembles of oligosaccharides, considering their minor conformers in a systematic manner.
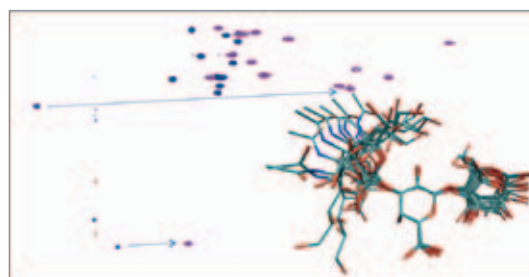
Figure 1. ^{1}H–^{13}C HSQC spectral change of the GM3 trisaccharide tagged with a paramagnetic ion and snapshots of the sugar from an MD-simulated trajectory.

## 2. Structural Basis for Improved Effector Functions of Antibodies by Engineering of Their Glycans

More than half of proteins in nature are estimated to be modified by sugar chains, which affect the physical and biological properties of proteins. The effector functions of immunoglobulin G (IgG) critically depend on *N*-glycosylation of its Fc region. Removal of the fucose residue from the *N*-glycans of IgG-Fc results in a dramatic enhancement of antibody-dependent cellular cytotoxicity (ADCC) through improved affinity for Fcγ receptor IIIa (FcγRIIIa). We successfully determined the crystal structure of the complex formed between non-fucosylated IgG1-Fc and a soluble form of FcγRIIIa (sFcγRIIIa) with two *N*-glycosylation sites (Figure 2a).[3] The crystal structure demonstrates that one of the two *N*-glycans of sFcγRIIIa mediates the interaction with the *N*-glycan of non-fucosylated Fc, thereby stabilizing the complex. However, fucosylation of the Fc *N*-glycans impairs this interaction because of steric hindrance. On the other hand, our NMR data demonstrated that Tyr296 of the non-fucosylated Fc glycoform exhibits conformational multiplicity in its un-complexed state, suggesting that conformational selection is governed by the presence or absence of the fucose residue of the Fc *N*-glycan. These findings offer a structural basis for improvement in ADCC of therapeutic antibodies by defucosylation.

3. Conformational Dynamics of Proteins Involved in the Ubiquitin-Proteasome System

While recent progresses have been made in understanding intra-domain conformational fluctuations of proteins, the evaluation of the relative motions of individual domains of multi-domain proteins is still a challenge. We successfully characterized conformational dynamics of Lys-48-linked Ub dimer (diUb) in solution using NMR spectroscopy.[4] Comparison of a chemical shift of wild-type diUb with that of monomeric Ub and cyclic diUb, which mimic the open and closed states (Figure 2b), respectively, with regard to the exposure of hydrophobic surfaces to the solvent indicates that wild-type Lys-48-linked diUb in solution predominantly exhibits the open conformation (75% at pH 7.0), which becomes more populated upon lowering pH. The intrinsic properties of Lys-48-linked Ub chains to adopt the open conformation may be advantageous for interacting with Ub-binding proteins. We also characterized interaction modes of the Ub-like domains of HOIL-1L and HR23 with their specific binding-partners by NMR spectroscopy.[5,6]

Furthermore, we developed a novel technique for real-time monitoring of subunit exchange in homooligomeric proteins, using deuteration-assisted small-angle neutron scattering, and applied it to the tetradecamer of the proteasome α7 subunit.[7]
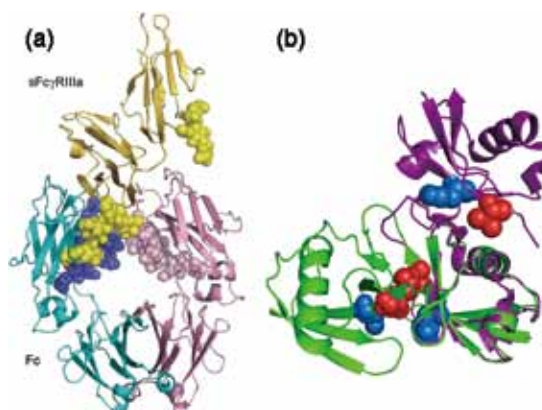
Figure 2. 3D structures of (a) sFcγRIIIa bound to non-fucosylated Fc and (b) wild-type Lys-48-linked diUb. The open form of diUb (purple) was superposed on the closed state (green).

References

1) S. Yamamoto, Y. Zhang, T. Yamaguchi, T. Kameda and K. Kato, *Chem. Commun.* **48**, 4752–4754 (2012).

2) Y. Zhang, S. Yamamoto, T. Yamaguchi and K. Kato, *Molecules* **17**, 6658–6671 (2012).

3) T. Mizushima, H. Yagi, E. Takemoto, M. Shibata-Koyama, Y. Isoda, S. Iida, K. Masuda, M. Satoh and K. Kato, *Genes Cells* **16**, 1071–1080 (2011).

4) T. Hirano, O. Serve, M. Yagi-Utsumi, E. Takemoto, T. Hiromoto, T. Satoh, T. Mizushima and K. Kato, *J. Biol. Chem.* **286**, 37496–37502 (2011).

5) H. Yagi, K. Ishimoto, T. Hiromoto, H. Fujita, T. Mizushima, Y. Uekusa, M. Yagi-Utsumi, E. Kurimoto, M. Noda, S. Uchiyama, F. Tokunaga, K. Iwai and K. Kato, *EMBO Rep.* **13**, 462–468 (2012).

6) Y. Kamiya, Y. Uekusa, A. Sumiyoshi, H. Sasakawa, T. Hirao, T. Suzuki and K. Kato, *FEBS Lett.* **586**, 1141–1146 (2012).

7) M. Sugiyama, E. Kurimoto, H. Yagi, K. Mori, T. Fukunaga, M. Hirai, G. Zaccai and K. Kato, *Biophys. J.* **101**, 2037–2042 (2011).

* Present Address; Graduate School of Engineering, Nagoya University

† carrying out graduate research on Cooperative Education Program of IMS with Nagoya City University

‡ carrying out graduate research on Cooperative Education Program of IMS with Kasetsart University

Structure-Function Relationship of Metalloproteins

Department of Life and Coordination-Complex Molecular Science
Division of Biomolecular Functions

FUJII, Hiroshi	Associate Professor
KURAHASHI, Takuya	Assistant Professor
CONG, Zhiqi	IMS Fellow
OHTSUKI, Akimichi	Post-Doctoral Fellow
WANG, Chunlan	Graduate Student
TANIZAWA, Misako	Secretary

Metalloproteins are a class of biologically important macromolecules, which have various functions such as oxygen transport, electron transfer, oxidation, and oxygenation. These diverse functions of metalloproteins have been thought to depend on the ligands from amino acid, coordination structures, and protein structures in immediate vicinity of metal ions. In this project, we are studying the relationship between the electronic structures of the metal active sites and reactivity of metalloproteins.

1. Formation of Iron(III) *Meso*-Chloro-Isoporphyrin as a Reactive Chlorinating Agent from Oxoiron(IV) Porphyrin π-Cation Radical[1]

Oxoiron(IV) porphyrin π-cation radicals are generally known to function as key reactive intermediates in a variety of oxidation reactions catalyzed by heme enzymes such as cytochrome P450. The oxoiron(IV) porphyrin π-cation radical complex has several isoelectronic forms which are two oxidation state equivalents higher than that of the iron(III) porphyrin complex. Isoporphyrins, tautomers of porphyrins with a saturated *meso* carbon, were originally postulated by Woodward, and its metal complex was first reported by Dolphin *et al.*, who prepared a zinc(II) 5'-methoxy-5,10,15,20-tetraphenyl-isoporphyrin complex by nucleophilic attack of methanol on zinc(II) 5,10,15,20-tetraphenylporhyrin π-dication complex. Since then, iron(III) isoporphyrin complexes, particularly *meso*-tetraaryl derivatives, have been synthesized chemically and electrochemically. However, to our surprise, atom transfer reactions of isoporphyrin complexes to substrates, such as oxygenation and halogenation reactions, have not been studied well. In this study, we show that an oxoiron(IV) π-cation radical complex can be converted to iron(III) *meso*-chloro-isoporphyrin complex in the presence of trifluoroacetic acid (TFA) and chloride ion. The formation of the isoporphyrin complex would be due to protonations of the oxo ligand of oxoiron(IV) porphyrin π-cation radical species. More impor-

tantly, this study shows that the iron(III) *meso*-chloro-iso-porphyrin complex is a reactive reagent for chlorination of aromatic compounds and olefins.
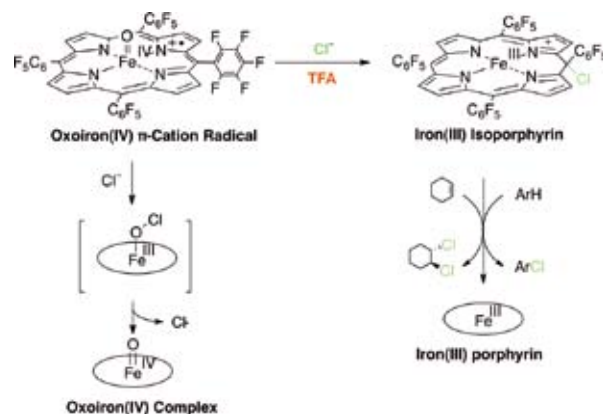
Figure 1. Reaction of oxoiron(IV) porphyrin π-cation radical complex with chloride ion in the presence and absence of proton.

2. The Effect of the Axial Ligand on the Reactivity of the Oxoiron(IV) Porphyrin π-Cation Radical Complex: Higher Stabilization of the Product State Relative to the Reactant State[2]

The proximal heme axial ligand plays an important role in tuning the reactivity of oxoiron(IV) porphyrin π-cation radical species (compound I) in enzymatic and catalytic oxygenation reactions. To reveal an essence of the axial ligand effect on the reactivity, we investigated from a thermodynamic viewpoint. Compound I model complexes, $(TMP^{+\bullet})Fe^{IV}O(L)$ (where TMP is 5,10,15,20-tetramesitylporphyrin and $TMP^{+\bullet}$ is its π-cation radical), can be provided with altered reactivity by changing the identity of the axial ligand, but the reactivity is not correlated with spectroscopic data ($\nu(Fe=O)$, redox potential, and so on) of $(TMP^{+\bullet})Fe^{IV}O(L)$. Surprisingly, a clear correlation was found between the reactivity of $(TMP^{+\bullet})$
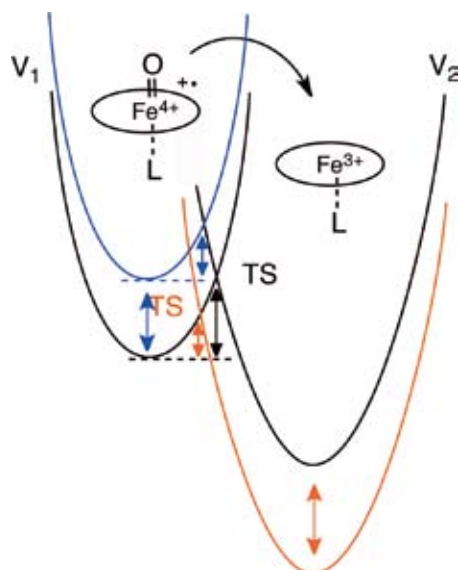
Figure 2. Curve crossing diagram of potential-energy surfaces of the reactant, $(TMP^{+\bullet})Fe^{IV}O(L)$, and product, $(TMP)Fe^{III}(L)$, states. Blue line; Change of stability of $(TMP^{+\bullet})Fe^{IV}O(L)$ and red line; change of stability of $(TMP)Fe^{III}(L)$.

$Fe^{IV}O(L)$ and the Fe^{II}/Fe^{III} redox potential of $(TMP)Fe^{III}L$, the final reaction product. This suggests that the thermodynamic stability of $(TMP)Fe^{III}L$ is involved in the mechanism of the axial ligand effect. Axial ligand-exchange experiments and theoretical calculations demonstrate a linear free-energy relationship, in which the axial ligand modulates the reaction free energy by changing the thermodynamic stability of $(TMP)Fe^{III}(L)$ to a greater extent than $(TMP^{+\bullet})Fe^{IV}O(L)$. The linear free energy relationship could be found for a wide range of anionic axial ligand and for various types of reactions, such as epoxidation, demethylation, and hydrogen abstraction reactions. An essence of the axial ligand effect is neither the electron donor ability of the axial ligand nor the electron affinity of compound I, but the binding ability of the axial ligand (the stabilization by the axial ligand). An axial ligand that binds more strongly makes $(TMP)Fe^{III}(L)$ more stable and $(TMP^{+\bullet})Fe^{IV}O(L)$ more reactive. All results indicate that the axial ligand controls the reactivity of compound I (the stability of the transition state) by the stability of the ground state of the final reaction product and not by compound I itself.

3. Oxidation of Chloride Ion and Subsequent Chlorination of Organic Compounds by Oxoiron(IV) Porphyrin π-Cation Radical Complexes[3)]

Enantioselective transition-metal-catalyzed oxygenation

reactions have received much attention because of the demand for organic synthesis strategies and their biological relevance with respect to metalloenzymes. Terminal oxidants such as peroxides, iodosylarenes, and peracids have been utilized as an oxygen source for these oxygenation reactions. Since the terminal oxidants must be stable for easy handling, the primary role of the transition-metal catalyst is to activate a stabilized oxidant and to generate a transient species that remains active enough to transfer an oxygen atom to a substrate. The activation of a terminal oxidant is initiated by binding to the metal complex to form a terminal oxidant adduct of the metal complex. Recently, evidence has been mounting in support of the proposal that the terminal oxidant adduct of a metal complex is not only a precursor to a reactive high valent metal-oxo species, but also itself may serve as a reactive species for an oxygenation reaction. Although terminal oxidant adducts of metal complexes are unstable and reactive compounds in most cases, metal complex adducts with hydrogen peroxide, alkylperoxides, and *m*-CPBA have been isolated and structurally characterized. In contrast to these successful reports, and much to our surprise, there have been no examples of structural characterization of any iodosylarene adducts of metal complexes, although they have emerged as useful oxidants for various organic reactions. The most intensive spectroscopic study was performed by Hill *et al.*, who thoroughly investigated an iodosylbenzene adduct of a manganese porphyrin complex with ^{1}H NMR, IR and [127]I Mössbauer spectroscopy. However, the nature of the bonding interaction between iodosylbenzene and the metal ion remains unclear. Here, we report on the preparation and X-ray crystal structure of an iodosylarene adduct of a manganese(IV) salen complex bearing a *trans*-cyclohexane-1,2-diamine linkage as chiral unit.

Figure 3. Synthesis and structural characterization of bis-iodosyl-mesitylene adduct of manganese(IV) salen complex.

References
1) Z. Cong, T. Kurahashi and H. Fujii, *J. Am. Chem. Soc.* **134**, 4469–4472 (2012).

2) A. Takahashi, D. Yamaki, K. Ikemura, T. Kurahashi, T. Ogura, M. Hada and H. Fujii, *Inorg. Chem.* **51**, 7296–7305 (2012).

3) C. Wang, T. Kurahashi and H. Fujii, *Angew. Chem., Int. Ed.* **51**, 7809–7811 (2012).

Award

Molecular Origin of 24 Hour Period in Cyanobacterial Protein Clock

Department of Life and Coordination-Complex Molecular Science
Division of Biomolecular Sensing

AKIYAMA, Shuji   Professor (April, 2012–)
ABE, Hitomi   Secretary

Circadian (approximately 24 h) clocks are endogenous time-keeping systems encapsulated in living cells, enabling organisms to adapt to daily fluctuation of exogenous environments on the Earth. These time-keeping systems, found ubiquitously from prokaryotes to eukaryotes, share the three characteristics. First, the circadian rhythmicity of the clocks persists even without any external cues (self-sustainability). Second, the period is little dependent on ambient temperature (temperature compensation). Third, the phase of the clock can be reset by external stimuli such as lightning, humidity, or temperature so as to be synchronized to the external phase (synchronization).

KaiC, a core protein of the circadian clock in cyanobacteria, undergoes rhythmic structural changes over approximately 24 h in the presence of KaiA and KaiB (Kai oscillator). This slow dynamics spanning a wide range of both temporal and spatial scales is not well understood, and is central to a fundamental question: what determines the temperature-compensated 24 h period?[1,2] The Kai oscillator reconstitutable *in vitro* is advantageous for studying its dynamic structure through a complementary usage of both X-ray crystallography and solution scattering, its transient response by using physicochemical techniques, and its molecular motion through a collaborative work with computational groups.

Our mission is to explore the frontier in molecular science of the cyanobacterial circadian clock from many perspectives. This Annual Report summarizes our recent activities from April 1, 2012 through August 31, 2012.

## 1. Tracking the Ticking of Cyanobacterial Clock Protein KaiC in Solution[3]

The ATPase activity of KaiC *alone* is strongly correlated with the oscillatory period of the Kai oscillator. This correlation suggests that the ATPase activity of KaiC is one of the period-determining factors of the Kai oscillator. Hence, the determination of the structural change of KaiC interlocked with the ATPase activity is of great of importance.
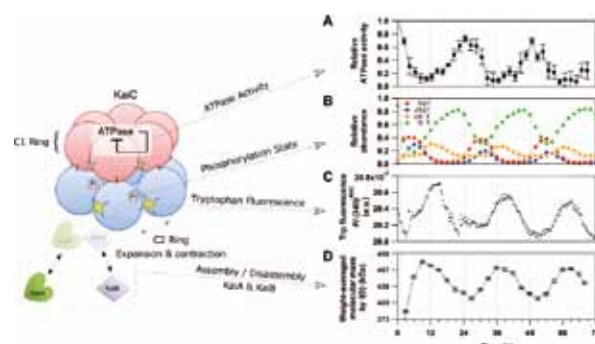
Figure 1. Circadian dynamics of cyanobacterial clock protein KaiC. The C1 and C2 domains in each protomer of KaiC are drawn as red and blue spheres, respectively. Expansion and contraction motions of the C2 ring (B, C) in solution serves as a timing cue for assembly/disassembly of KaiA and KaiB (D), and is interlocked with its C1 ATPase udder a control of negative-feedback regulation (A).

To track the dynamic transition of KaiC in real-time, we recorded the time evolution of intrinsic tryptophan (Trp) fluorescence from KaiC contained in the Kai oscillator. KaiC is a dumbbell-shaped molecule composed of tandemly duplicated N-terminal (C1) and C-terminal (C2) domains. Six protomers are assembled into a hexamer to attain a double-doughnut shape. Two tryptophan (Trp) residues located in the protomer-protomer interface of the C2 domain can serve as a sensitive probe to monitor the potential structural transition of the C2 ring. The intensity of the Trp fluorescence from KaiC revealed a rhythmic fluctuation with the period of approximately 24 h (Figure 1, panel C). So far as we know, this is the first experimental evidence that demonstrated a dynamic
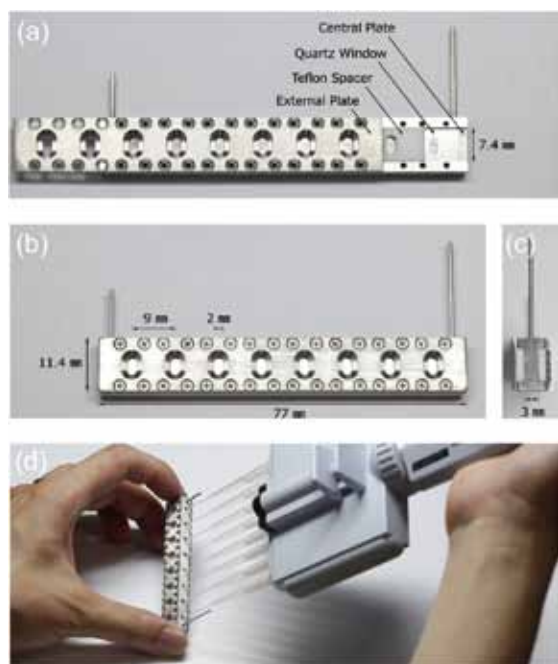
Figure 2. Octuple cuvette. (a) Photograph of the central plate covered by the quartz window, Teflon spacer and external plate, in that order. (b) Front view of the assembly. (c) Side view of the assembly. (d) Filling and removal of solutions using a commercially available eight-channel pipette. The sample volume of each chamber is 25 μl.

structural transition of the C2 ring of KaiC in solution.

Concomitantly with the Trp-fluorescence dynamics, KaiC underwent a periodic change in its phosphorylation state (Figure 1, panel B). KaiC has the two phosphorylation sites, *i.e.*, Ser431 and Thr432, in the C2 domain, and both residues are phosphorylated and then dephosphorylated in a programmed sequence during the phosphorylation cycle as follows: KaiCS/pT → KaiCpS/pT → KaiCpS/T → KaiCS/T (where 'S' represents Ser431, 'pS' represents phosphorylated Ser431, 'T' represents Thr432, and 'pT' represents phosphorylated Thr432). Interestingly, the Trp fluorescence was maximized at the timing when the KaiCpS/T state was populated (Figure 1, panels B and C). The result suggests the Trp fluorescence is an excellent measure of the phosphor-coupled transition of the C2 ring in KaiC.

2. Visualization of Dynamic Structural Changes of KaiC Using Small-Angle X-Ray Solution Scattering Technique[3,4]

To visualize the C2-ring dynamics confirmed by tracking Trp fluorescence, we measured the small-angle x-ray scattering (SAXS) from KaiC in solution. To obtain the SAXS data of biological samples in solution, one must first record the scattering intensity of the sample (biomacromolecules in solution) and then that of the matching buffer in the separate
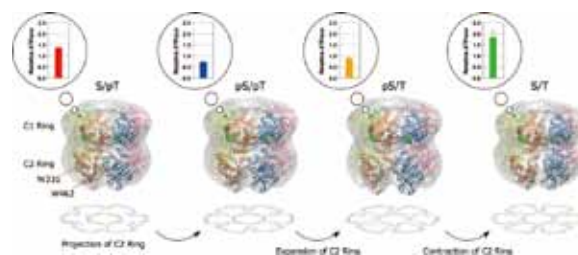
Figure 3. Expansion and contraction motions of C2 ring of KaiC interlocked with ATPase activity.

experiment, and finally find the difference between two intensities. The cuvette used for conventional SAXS experiments has only a single observation chamber in order to ensure the qualitative subtraction of the scattering contributed by the solvent molecules. On the other hand, the use of the single-chamber cuvette makes both the experiment and analysis time-consuming.

To record the SAXS pattern of KaiC both efficiently and qualitatively, we designed and constructed an eight-chamber cuvette (octuplet cuvette), each chamber of which was fabricated so uniformly to ensure the inter-chamber subtraction (Figure 2). The developed cuvette enabled us to acquire SAXS dataset of KaiC roughly 10 times faster without any significant degradation of data quality.

On the basis of the obtained SAXS data, we built low-resolution models of the KaiC hexamer as shown in Figure 3. The overall shape is almost unchanged in the transition from KaiCS/pT to KaiCpS/pT, whereas the radius of the C2 ring is dramatically enlarged in the subsequent transition from KaiCpS/pT to KaiCpS/T. The expanded C2 ring is partly contracted in the transition from KaiCpS/T to KaiCS/T, and is further contracted in the subsequent transition from KaiCS/T to KaiCS/pT. The present model suggests that KaiC ticks through expanding and contracting motions of the C2 ring.

The dynamic motion of the C2 ring uncovered throughout our study is chronobiologically meaningful, we believe, in terms of the elucidation of the key conformational change tightly coupled to the period-determining ATPase of KaiC. Our group is trying to improve spatio-temporal resolution of the experiments so as to draw a more dynamic and detailed picture of KaiC ATPase.

References

1) S. Akiyama, *Cell. Mol. Life Sci.* **69**, 2147–2160 (2012).
2) A. Mukaiyama, T. Kondo and S. Akiyama, *SPring-8 Research Frontiers 2011* 47–48 (2012).
3) Y. Murayama, A. Mukaiyama, K. Imai, Y. Onoue, A. Tsunoda, A. Nohara, T. Ishida, Y. Maéda, T. Kondo and S. Akiyama, *EMBO J.* **30**, 68–78 (2011).
4) S. Akiyama and T. Hikima, *J. Appl. Crystallogr.* **44**, 1294–1296 (2011).

Investigation of Molecular Mechanisms of Channels, Transporters and Receptors in Membrane

Department of Life and Coordination-Complex Molecular Science
Division of Biomolecular Sensing

FURUTANI, Yuji	Associate Professor
KIMURA, Tetsunari	Assistant Professor
TSUKAMOTO, Hisao	IMS Research Assistant Professor
INAGUMA, Asumi	Post-Doctoral Fellow
GUO, Hao	Graduate Student
FUJIWARA, Kuniyo	Graduate Student
SHIMIZU, Atsuko	Secretary

Membrane proteins are important for homeostasis of living cells, which work as ion channels, transporters, various types of chemical and biophysical sensors, and so on. These proteins are considered as important targets for biophysical studies.

Our main goal is to clarify molecular mechanisms of channels, transporters and receptors in cell membrane mainly by using stimulus-induced difference infrared (IR) spectroscopy, which is sensitive to the structural and environmental changes of organic- and bio-molecules. Recently, Dr. Kimura started to construct a microfluidic device to monitor biological and chemical reactions by infrared and fluorescent microscopic techniques. Dr. Tsukamoto has established a protein expression system with mammalian cell line.

1. Anion-Transport Mechanism of a Chloride Ion Pump *p*HR Studied by Time-Resoved FTIR Spectroscopy

pharaonis Halorhodopsin (*p*HR) is a light-driven inward chloride ion pump protein. The ion transportation is performed through the sequential formation of several intermediates (K, L_1, L_2, N and O) during the photocyclic reaction. The structural details of each intermediate state have been studied by various kinds of physicochemical methods, however it is still open question how the structural changes of protein molecule and water molecules are involved in the translocation of a chloride ion inside protein at physiological temperature. To analyze the structural dynamics, we performed the time-resolved Fourier transform infrared (TR-FTIR) spectroscopy in the whole mid-infrared region under various hydration conditions. Measurements under D_2O reveal the structural information of the water inaccessible backbone of protein itself, and those with H_2O or $H_2^{18}O$ give an insight on the dynamics of water molecules inside protein. We concluded that the chloride ion release and uptake occurring in the N and O intermediate states are accompanied by the drastic conformational changes in the water-inaccessible transmembrane-

helices and the hydrogen- bonding network rearrangement of the internal water molecules in *p*HR (*manuscripts in preparation*).

2. Time-Resolved Difference FTIR Spectroscopy Triggered by Rapid Buffer-Exchange

Attenuated total reflection (ATR) FTIR spectroscopy is a powerful technique to obtain infrared spectra of membrane proteins immersed in aqueous solution.[1] By exchanging buffer with and without salts, the difference spectra between the two conditions provide the structural information relating to the interaction between protein and ions. In this year, we executed the construction of the kinetic ATR FTIR spectroscopic system, which can follow the chemical and biological reaction triggered by the rapid buffer-exchange, in collaboration with Mr. K. Okamoto in UNISOKU Co. Ltd.

We have developed the photo-triggering system for time-resolved FTIR measurements, but the application of this system has been limited mainly to the photo-inductive chemical reactions. Rapid buffer exchange (<1 ms) allows us to monitor the early stage of reactions, such as substrate or ion binding. For further improvement of the time-resolution, we will construct the flow-flash system.


Figure 1. Picture of the rapid buffer-exchange system.

3. Development of a Microfluidic Device to Monitor Biological and Chemical Reactions

Real-time observation is one of the powerful techniques to understand the molecular mechanisms of the self-organization

and molecular association. The solution mixing technique realizes many reaction fields for biological and chemical reactions by changing the buffer condition and can be combined with spectroscopic equipment easily. However, conventional mixing techniques limit their targets because of the large consumption of the sample and the stress of the turbulent mixing. We are developing a novel microfluidic device and trying to reduce both the sample consumption to ~1/1000 and the stress by using sheath flow.
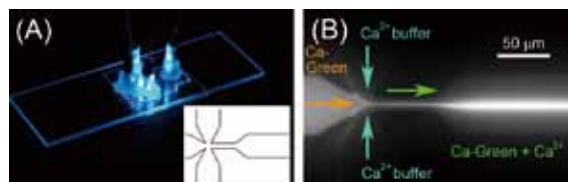
Figure 2. Pictures of the developed microfluidic mixer. (A) Picture of the mixer on the XY-stage of the fluorescence microscope. (inset) Schematic figure of the designed flow channels. (B) Fluorescence image of the Ca-Green mixed with the Ca^{2+} buffer.

Microfluidic devices with the flow channels of micrometer scale are made of a single cast of poly(dimethylsiloxane), PDMS, with the photolithography technique. These devices were combined with the fluorescence microscope and the complete mixing with the time resolution of ~20 μs was confirmed by the fluorescent intensity measurements. We are attempting to combine these devices with FTIR or other fluorescence spectroscopy.

The devices were manufactured with the strong supports of Equipment Development Center of IMS (especially Ms. N. Takada and Mr. M. Aoyama).

4. Investigation of Membrane Proteins Which Are Hardly Expressed in *E. coli*

Heterologous expression system using *E. coli* is established and easy way to obtain large amount of purified proteins, but in general, expression of membrane proteins, in particular mammalian ones, is very difficult. In this year, we have tried to establish a protein expression system using cultured mammalian cells for IR spectroscopic analyses of various membrane proteins, including mammalian ones.

In order to study structure-function relationship using purified proteins, it is very important to select target proteins that can be highly expressed in cell lines. Traditionally the screening of membrane proteins is very painful and time-consuming. However, a powerful method named fluorescence-detected size-exclusion chromatography (FSEC) was recently developed (Kawate and Gouaux, 2006). FSEC method evaluates expression level and properties of target proteins using GFP-tag and size-exclusion chromatograph even without purification (Figure 3). We set up an FSEC system and
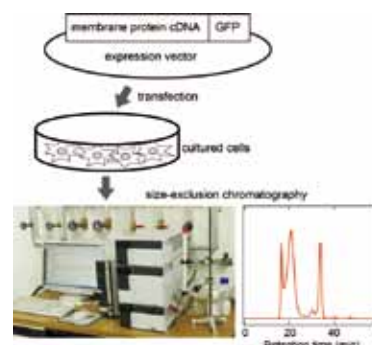
Figure 3. Scheme of the fluorescence-detected size-exclusion chromatography (FSEC).

expressed various membrane proteins with GFP tag to select appropriate proteins. Also, we tried to purify screened proteins and apply them to IR spectroscopic analyses.

Channelrhodopsins (collaboration with Prof. Yawo's group in Tohoku Univ.)

Channelrhodopin is a light-gated cation channels, which is originally identified in *Chlamydomonas*. Currently this protein is used as a tool for "optogenetics" which enables excitation of specific neural cells by irradiation. Prof. Yawo's group has developed several interesting channelrhodopsin mutants that show unique electrophysiological properties. Prof. Yawo kindly provided constructs of the channelrhodopsin mutants to us, and we screened the mutants using FSEC method. Several mutants can be expressed efficiently in mammalian cells, and can be purified. Also, we have already succeeded to measure the difference IR spectra before and after photo-activation of the channelrhodopsins. We are now trying to analyze the spectra and extend to time-resolved measurements with 12.5 μs resolution to reveal real-time analyses of open-close mechanism of the channel protein. (collaboration with Prof. Nureki's group in Univ. of Tokyo)

Mammalian potassium channels (collaboration with Prof. Kubo's group in National Institute for Physiological Sciences (NIPS))

Mammalian potassium channels play important roles in various organs, including brain, heart, kidney and retina. Prof. Kubo's group has revealed structure-function relationship of these channels mainly using electrophysiological method. Prof. Kubo kindly provided constructs of various mammalian potassium channels to us. We tested properties of these channels expressed in cultured cells using FSEC, and found several inwardly rectifying potassium channels can be expressed efficiently and show appropriate properties. In addition, we have just successfully purified the channels. Currently we are trying to measure IR spectra of the purified channels.

Reference

1) Y. Furutani, T. Murata and H. Kandori, *J. Am. Chem. Soc.* **133**, 2860–2863 (2011).

Heterogeneous Catalytic Systems for Organic Chemical Transformations in Water

Department of Life and Coordination-Complex Molecular Science
Division of Complex Catalysis

UOZUMI, Yasuhiro	Professor
OSAKO, Takao	Assistant Professor
HAMASAKA, Go	Assistant Professor
ZHOU, Haifeng	Post-Doctoral Fellow
KOBAYASHI, Noboru	Graduate Student
SAKURAI, Fumie	Graduate Student
TSUJI, Hiroaki	Graduate Student
ITO, Kenichi	Graduate Student
TORII, Kaoru	Technical Fellow
SASAKI, Tokiyo	Secretary
FUKUSHIMA, Tomoko	Secretary

Various transition metal-catalyzed organic molecular transformations in water were achieved under heterogeneous conditions by use of poly(imidazole-palladium), amphiphilic resin-supported palladium complexes, or a microflow device containing a polymeric palladium nanoparticle membrane which were designed and prepared by this research group. The enantioselective carbenoid insertion into phenolic O–H bonds with a new chiral copper(I) imidazoindolephosphine complex has been also developed. In particular, development of a highly active reusable poly(imidazole-palladium) and a microflow device containing a plolymeric Pd nanoparticle membrane for organic transformations in water and the highly enantioselective O–H insertion using a new chiral copper(I) complex are highlights among the achievements of the 2011–2012 period to approach what may be considered ideal chemical processes of next generation. Representative results are summarized hereunder.

1. Self-Assembled Poly(Imidazole-Palladium): A Highly Active, Reusable Catalyst[1,2]

A polymeric imidazole Pd catalyst (MEPI-Pd) was readily prepared by the coordinative convolution of $(NH_4)_2PdCl_4$ and poly[(N-vinylimidazole)-co-(N-isopropylacrylamide$_5$)] in a methanol/water solution at 80 °C for 30 min. The polymeric Pd catalyst was utilized for the allylic arylation/alkenylation/vinylation of allylic esters and carbonates with aryl/alkenylboronic acids, vinylboronic acid esters, and tetraaryl borates. Even 0.8–40 mol ppm Pd of the catalyst efficiently promoted allylic arylation/alkenylation/vinylation in alcohol and/or water with a catalytic turnover number (TON) of 20,000–1,250,000. Furthermore, the polymeric Pd catalyst efficiently promoted the Suzuki-Miyaura reaction of a variety of inactivated aryl chlorides, as well as aryl bromides, and iodides in water with a TON of up to 3,570,000.
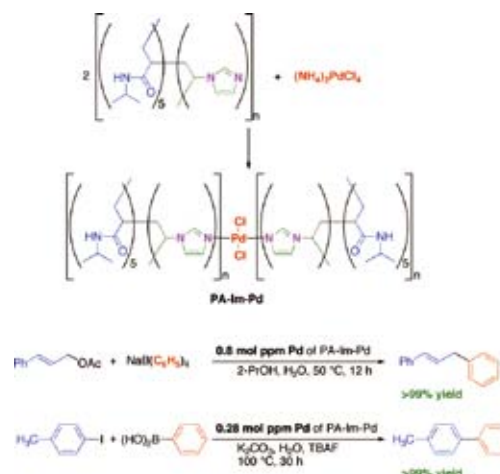

Scheme 1. Preparation of Self-Assembled Poly(Imidazole-Palladium) (top) and Application to Allylic Arylation and Suzuki-Miyaura Reaction.

2. Instantaneous Hydrodehalogenation of Haloarenes by a Microflow Device Containing a Polymeric Pd Nanoparticle Membrane[3]

An architecture-based system of transition metal catalysis usinWe developed a variety of polymeric Pd nanoparticle membrane-installed microflow devices for the first time. Three types of polymers were convoluted with palladium salts under laminar flow conditions in a microflow reactor to form polymeric Pd membranes at the laminar flow interface. These

membranes were reduced with aqueous sodium formate or with heat to create microflow devices containing polymeric palladium nanoparticle membranes. These microflow devices achieved instantaneous hydrodehalogenation of 10–1,000 ppm of aryl chlorides, bromides, iodides, and triflates, within a residence time of 2–8 s at 50–90 °C using a safe, nonexplosive aqueous sodium formate to quantitatively afford the corresponding hydrodehalogenated products. PCB (10–1,000 ppm) and PBB (1,000 ppm) were completely decomposed under similar conditions, yielding biphenyl as a fungicidal compound.
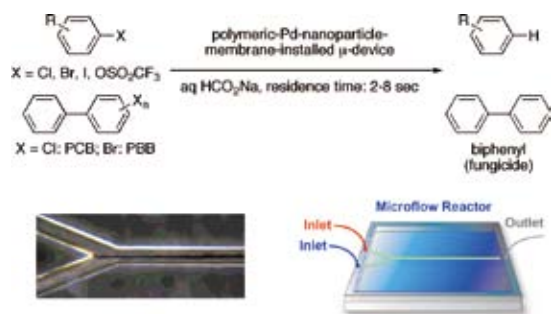
Scheme 2. Instantaneous Hydrodehalogenation of Haloarenes by a Microflow Device Containing a Polymeric Pd Nanoparticles Membrane.

3. C–N and C–S Bond Forming Cross Coupling in Water with Amphiphilic Resin-Supported Palladium Complexes[4)]

Catalytic C–N and C–S bond forming reactions of haloarenes with secondary amines and thiophenols were achieved in water under heterogeneous conditions by the use of immobilized palladium complexes coordinated with the amphiphilic polystyrene-poly(ethylene glycol) resin-supported di(*tert*-butyl)phosphine ligand to afford aryl(dialkyl)amines and diarylsulfides in high yield.
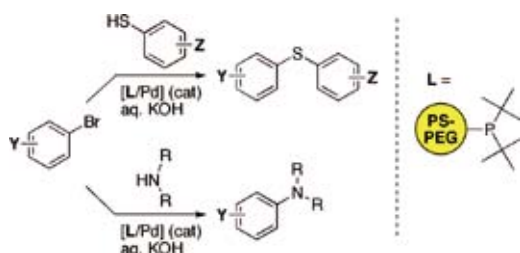
Scheme 3. C–N and C–S Bond Forming Cross Coupling in Water with Amphiphilic Resin-Supported Pd Complexes.

4. Enantioselective Carbenoid Insertion into Phenolic O–H Bonds with a Chiral Copper(I) Imidazoindolephosphine Complex[5)]

The enantioselective O–H carbenoid insertion reaction with a new chiral copper(I) imidazoindolephosphine complex has been developed. The chiral copper(I) complex catalyzed the insertion of carbenoids derived from α-diazopropionates into the O–H bonds of various phenol derivatives to give the corresponding α-aryloxypropionates with up to 91% ee.
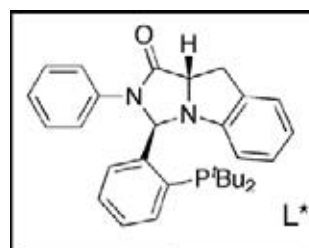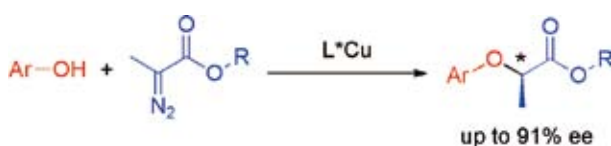
Scheme 4. Enantioselective Carbenoid Insertion into Phenolic O–H Bonds with a Chiral Copper(I) Imidazoindolephosphine Complex.

References

1) S. M. Sarkar, Y. Uozumi and Y. M. A. Yamada, *Angew. Chem., Int. Ed.* **50**, 9437–9441 (2011).

2) Y. M. A. Yamada, S. M. Sarkar and Y. Uozumi, *J. Am. Chem. Soc.* **134**, 3190–3198 (2012).

3) Y. M. A. Yamada, T. Watanabe, A. Ohno and Y. Uozumi, *ChemSusChem* **5**, 293–299 (2012).

4) Y. Hirai and Y. Uozumi, *Chem. Lett.* **40**, 934–935 (2011).

5) T. Osako, D. Panichakul and Y. Uozumi, *Org. Lett.* **14**, 194–197 (2012).

Water Oxidation Catalyzed by Dimeric Ru Complexes

Department of Life and Coordination-Complex Molecular Science
**Division of Functional Coordination Chemistry**

TANAKA, Koji	Professor (–March, 2012)*
OHTSU, Hideki	Assistant Professor*
KOBAYASHI, Katsuaki	IMS Research Assistant Professor*
PADHI, Sumanta Kumar	Post-Doctoral Fellow
NAKANE, Daisuke	Post-Doctoral Fellow
YAMAGUCHI, Yumiko	Secretary
NOGAWA, Kyoko	Secretary

Artificial photosynthesis aimed at carbon dioxide reduction and water splitting has become a top research theme. Two-electron transfer from or to substrates through redox reactions is requisite for stable molecular transformation. Intermolecular electron transfer, however, always generates free radical species, which often causes undesired side reactions. Success of artificial photosynthesis, therefore, depends on the designing of reaction systems that can provide or take out multi-electrons to or from reaction centers.

Irradiation of $[Ru(bpy)_2(pbn)]^{2+}$ (pbn = 2-(2-pyridyl)-benzo[b]-1,5-naphthyridine) with visible light causes proton coupled one-electron reduction, and the subsequent disproportionation affords an NADH model complex, $[Ru(bpy)_2(pbnH_2)]^{2+}$ (pbnH$_2$ = 5,10-dihydro-2-(2-pyridyl)benzo[b]-1,5-naphthyridine) (Scheme 1). Smooth conversion from NAD analog to NADH one under visible light irradiation would lead to a new methodology for utilization of water as the hydrogen source in molecular transformation.
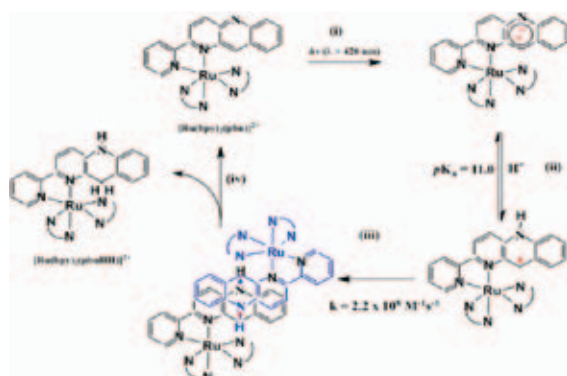
Scheme 1. Photochemical two-electron reduction of $[Ru(bpy)_2(pbn)]^{2+}$.

Three Ru-dioxolene complexes, $[Ru^{II}(Q)(trpy)(OH_2)]^{2+}$, $[Ru^{II}(Q)(trpy)(OH)]^+$, and $[Ru^{II}(Sq)(trpy)(O^{-\bullet})]^0$ (Q = 3,5-dibutylquinone; Sq = 3,5-dibutylsemiquinone) exist as equilibrium mixtures in water with the pK_a values of 5.5 and 10.5, respectively. A novel oxyl radical complex, $[Ru^{II}(Sq)(trpy)$
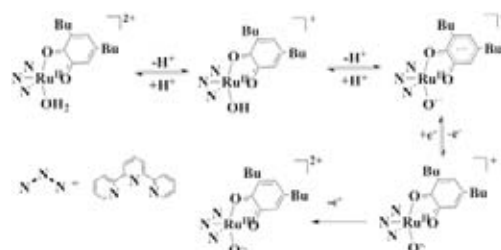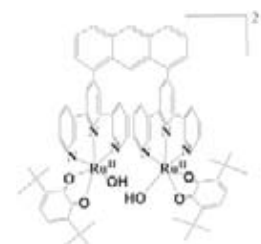

Scheme 2. Two-electron oxidant generation taking advantage of acid-base equilibrium of Ru-aqua(dioxolene) complex.

$(O^{-\bullet})]^0$, undergoes reversible one electron oxidation around 0 V (*vs.* Ag/AgCl), and the subsequent further one electron oxidation creates the unique Ru^{III}–O$^{-\bullet}$ framework in the product (Scheme 2). The oxyl radical and Ru(III) center involved in the product work as simultaneous hydrogen atom and one electron acceptors in two-electron oxidation of alcohols.

## 1. Direct Evidence for O–O Bond Formation in the Four Electron Water Oxidation

The difficulty of water decomposition results from four-electron oxiation of water rather than that of two-electron reduction. Among various water oxidation catalysts reported so far, much attention has been paid to a dinuclear Ru complex, $[Ru_2(OH)_2(Bu_2q)_2(btpyan)]^{2+}$ (Bu$_2$q = 3,6-di-*tert*-butylquinone, btpyan = 1,8-bis(terpyridyl)-anthracene), known as Tanaka Catalyst because of its high activity toward four-electron oxidation of water. However, any direct evidences for O–O bond formation prior to O$_2$ evolution have not been obtained so far. Four redox centers ($2 \times$ Ru$^{II/III}$ and $2 \times$ [Q]/[Sq]) of $[Ru_2(OH)_2$

$(Bu_2q)_2(btpyan)]^{2+}$ is attributable to the high catalytic capacity. So, we tried to detect the O–O bond formation process by decreasing the number of redox centers of an Ru dinuclear complex. Two-electron oxidation of $[Ru^{II}_2(Cl)_2(bpy)_2(btpyan)]^{4+}$ at +1.0 V in a range of pH 2.0 to 3.0 forms $[Ru^{IV}_2(=O)_2(bpy)_2(btpyan)]^{4+}$. The controlled potential electrolysis of $[Ru^{II}_2(\mu-Cl)(bpy)_2(btpyan)]^{3+}$ at +1.60 V in water at pH 2.6 (H_3PO_4/NaH_2PO_4 buffer) catalytically evolved dioxygen. Addition of a CH_3CN (100 µl) solution of $[Ru^{II}_2(\mu-Cl)(bpy)_2(btpyan)]^{3+}$ (1.0 µmol) into an aqueous solution (10 ml) of $Ce(NH_4)_2(NO_3)_6$ (2.5 mmol) at pH 1.0 (adjusted with HNO_3) also caused O_2 evolution (414 µmol).

The electronic absorption spectra of the reaction mixture showed a transient band at 688 nm that emerged only in O_2 evolution. The transient complex prepared by the electrolysis of $[Ru^{II}_2(\mu-Cl)(bpy)_2(btpyan)]^{3+}$ in $H_2^{16}O$ and $H_2^{18}O$ at +1.40 V displayed two absorption bands at 442 and 824 cm^{-1}, and 426 and 780 cm^{-1}, respectively, in the resonance raman spectra with irradiation at 633 nm. The isotope shifts (Δ 16 and 44 cm^{-1}) between $H_2^{16}O$ and $H_2^{18}O$ are quite consistent with the calculated values of the ν(Ru–O) and ν(O–O) bands of $[Ru_2(\mu-O_2)(bpy)_2(btpyan)]^{3+}$. If the $Ru^{IV}=O$ bond of $[Ru^{IV}_2(=O)_2(bpy)_2(btpyan)]^{4+}$ generated by the oxidation of $[Ru^{III}_2(OH)(bpy)_2(btpyan)]^{4+}$ has more or less Ru^{III}–O. oxyl radical character, $[Ru^{III}_2(\mu-O_2)(bpy)_2(btpyan)]^{4+}$ would be produced by the radical coupling of the two oxo groups of $[Ru^{IV}_2(=O)_2(bpy)_2(btpyan)]^{4+}$. The rate of O_2 evolution by chemical oxidation using Ce(IV) is much faster than that of electrochemical reaction at +1.60 V. Nuclear attack of two water to Ru^{III} of $[Ru^{III}_2(\mu-O_2)(bpy)_2(btpyan)]^{4+}$ will slowly releases O_2 (Scheme 3). On the other hand, Ce(IV) causes further oxidation of $[Ru^{III}_2(\mu-O_2)(bpy)_2(btpyan)]^{4+}$ to produce $[Ru^{IV}_2(\mu-O_2)(bpy)_2(btpyan)]^{6+}$, which smoothly evolves O_2 with regeneration of $[Ru^{III}_2(OH)(bpy)_2(btpyan)]^{4+}$ (Scheme 3). In accordance with this, $[Ru^{III}_2(\mu-O_2)(bpy)_2(btpyan)]^{4+}$ was detected only after Ce(IV) was consumed in O_2 evolution.
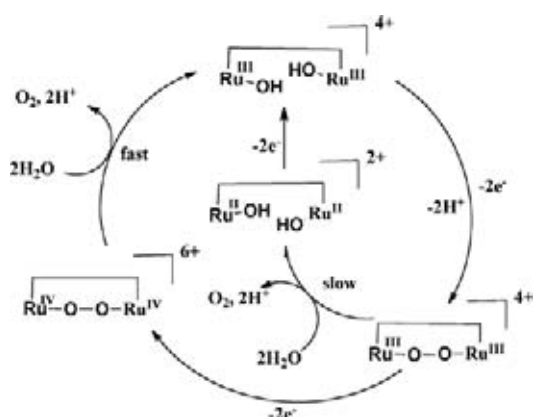
2. Insight for Activity of Tanaka Catalyst toward Water Oxidation

High catalytic ability of $[Ru_2(btpyan)(3,6\text{-}di\text{-}Bu_2Q)_2(OH)_2]^{2+}$ (Tanaka catalyst) toward water oxidation produces disputes about the electronic structures in the catalytic cycle. DFT computational works reported so far are not consistent with each other in the viewpoints of the relative stability between the closed-shell (Ru^{II}-Q) and open-shell (Ru^{III}-SQ) electronic structures, and the pathway to the O–O bond formation. On the other hand, broken-symmetry hybrid density functional computations have provided a rational reaction mechanism for water oxidation (Scheme 4). Deprotonation of waters in $^1\mathbf{1}$ affords the key tetraradical intermediate $^1\mathbf{3}$ via one-electron transfer (OET) in $^1\mathbf{2}$. The oxygen-radical pair in $^1\mathbf{3}$ is local triplet diradical (LTD), suppressing facile O–O bond formation by the radical coupling (RC) mechanism. The two-electron removal from $^1\mathbf{3}$ provides the hexaradical species $^3\mathbf{4}$. The oxygen radical pair (^{3}A) is still LTD-type, indicating the necessity of spin inversion (SI) for generation of local singlet diradical (LSD) pair in $^1\mathbf{5}$. The RC mechanism in $^1\mathbf{5}$ is facile, giving the peroxide species $^1\mathbf{6}$. The next step for generation of oxygen dianion may become the rate-determining step as shown in $^1\mathbf{7}$. The β-spin at the terminal oxygen anion in $^1\mathbf{7}$ is moved to the $Ru_2(III)$ site with the α-spin to form the singlet pair as shown in $^1\mathbf{8}$. The spin exchange (SE) between ↓•Ru_1(III) and SQ_1•↑ to generate ↑•Ru_1(III) and SQ_1•↓ is necessary for one more OET from superoxide anion to ↑•Ru_1(III) to afford triplet molecular oxygen in $^1\mathbf{9}$. The SE process is easy because the exchange coupling for the •O–O–Ru(III)• is weak. Thus the SQ_1• radical plays an important role for spin catalysis. The two-electron removal from $^1\mathbf{9}$ is necessary for reproduction of $^1\mathbf{1}$. Thus the BS computational results provide the orbital and spin correlation diagram for water splitting reaction.

Scheme 3. Four-electron oxidation of water catalyzed by $[Ru^{III}_2(OH)_2(bpy)_2(btpyan)]^{4+}$.
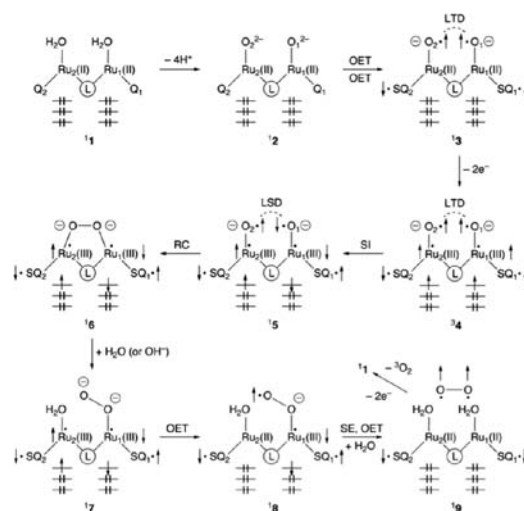
Scheme 4. Proposed mechanism for water oxidation catalyzed by Tanaka catalyst.

Synthetic Inorganic and Organometallic Chemistry of Transition Metals

Department of Life and Coordination-Complex Molecular Science
**Division of Functional Coordination Chemistry**

MURAHASHI, Tetsuro	Professor (April, 2012–)
TACHIBANA, Yuki	Graduate Student*
KIMURA, Seita	Graduate Student*
TANIWAKE, Mayuko	Secretary
NOGAWA, Kyoko	Secretary

Our research focuses on synthesis and structural elucidation of a new class of transition metal complexes. This research leads to development of fundamental concepts of transition metal chemistry as well as applications to catalysis and materials science. Novel synthetic methods are developed to realize transition metal complexes having unique bonding nature. The newly synthesized transition metal complexes are further converted to more reactive forms, and their reaction mechanisms are elucidated. The aspects gained by this research are applied to the understanding and development of molecular catalysis. Furthermore, unique properties of low-dimensional metal-organic hybrid molecules are investigated and developed in our group.

1. Synthesis and Chemical Properties of Metal Chain Sandwich Complexes

The molecular sandwich framework is one of the fundamental structures in transition metal chemistry. It had been believed that the structural concept can be applied only to mono- and dinuclear complexes. Our group revealed that the multinuclear sandwich complexes containing a one-dimensional metal chain or a two-dimensional metal sheet exist stably.[1,2] These findings expand the scope of the structural concept of sandwich compounds (Figure 1).
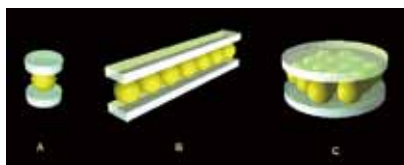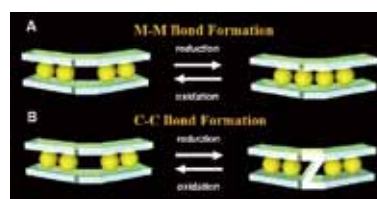

Figure 1. Schematic representation of sandwich compounds: (**A**) mononuclear metallocenes, (**B**) one-dimensional metal chain sandwich complexes, (**C**) two-dimensional metal sheet sandwich complexes. Our group revealed the existence of categories **B** and **C**.

For the one-dimensional metal chain sandwich complexes, we successfully developed a synthetic method that enables the size-selective construction of a metal chain sandwich framework. Furthermore, our laboratory revealed that metal chain sandwich complexes show unique chemical properties such as i) dynamic sliding behavior of polyene ligands on a metal chain and ii) photo-induced flipping of polyene ligands on a metal chain.

Redox-Switchable Metal Assembling and Ligand Coupling in Sandwich Frameworks[3]

In view of the widely developed redox chemistry of metallocenes and other mononuclear sandwich compounds, it is intriguing to elucidate the redox properties of the multinuclear sandwich compounds. Here we disclosed two novel modes of redox-induced reversible structural changes: i) redox-switchable reversible splitting of a Pd_4 chain via translocation, and ii) redox-switchable reversible C–C coupling of π-conjugated ligands in tetrapalladium sandwich complexes (Figure 2). These results provide new aspects for the redox function of (sp^2-carbon)–(multinuclear metal)–(sp^2-carbon) sandwich frameworks.


Figure 2. Schematic representations of (**A**) the reversible assembling of dimetal moieties and (**B**) the reversible coupling of ligands.

Oxidation of **1** or **1-OMe** with $AgBF_4$ or $AgPF_6$ (2 equiv.) resulted in the formation of **2** or **2-OMe** (bpbb = 1,2-bis(4-phenyl-1,3-butadienyl)benzene). Reduction of **2** or **2-OMe** with $Fe(C_5H_5)_2$ (2 equiv.) yielded **1** or **1-OMe** (eq. 1). During the two-electron oxidation, the Pd–Pd–Pd–Pd chain is cleaved, and the two Pd_2 units undergo translocation to the outer position during the oxidation process. In the reduction process, the two separate Pd_2 units migrate to the inside position to form the Pd–Pd–Pd–Pd chain. The observed redox behavior is highlighted by the coupling of two events, metal–metal bond formation/cleavage and metal translocation, under the redox control, and provides evidence of redox-switchable movement of multiple metal atoms associated with assembling/disas-

sembling behavior in the space between sp^2-carbon planes.

We also found another mode of the redox-induced structural change featured by the intramolecular reversible C–C bond formation between the two sandwich ligands, by employing **3** (eq. 2).
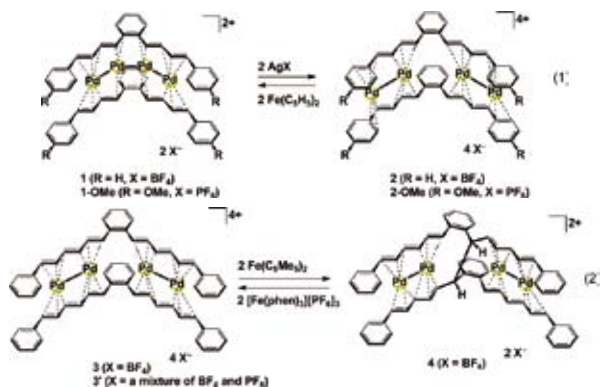

## 2. Synthesis and Reactivity of Metal Sheet Sandwich Complexes

For the two-dimensional metal sheet sandwich complexes, our group has shown that six-, seven-, eight-, and nine-membered carbocycles, as well as polycyclic arenes behave as the excellent binders for metal sheets. These metal sheet sandwich complexes are stable even in solution. Thus, a reactive form of such metal sheet sandwich complexes may provide a new opportunity to develop sandwich type late transition metal catalysts.

Selective Synthesis of Mixed Metal Pd₂Pt and PdPt₂ Complexes of Tropylium[4]

Our group has reported a series of homonuclear metal sheet sandwich complexes, which have a metal sheet of a single metal element. Here, we reported selective construction of the triangular $PdPt_2$ and Pd_2Pt cores in a common sandwich framework, where a key is to use different carbocyclic ligands for the different composite sandwich; *i.e.*, cycloheptatrienyl for $PdPt_2$, and cycloheptatriene for Pd_2Pt (complexes **5-PdPt₂** and **6-Pd₂Pt**).
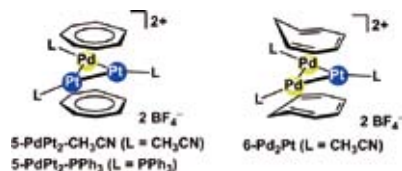
After construction of the Pd_2Pt core, the cycloheptatriene ligands can be converted to cycloheptatrienyl ligands where a (carbocyclic ligand)–(metal triangle)–(carbocyclic ligand) sandwich structure is retained (eq. 3). It was confirmed that the
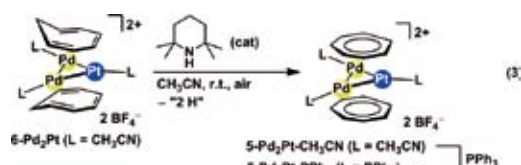
mixed metal core once formed in a cycloheptatrienyl sandwich framework is robust against the intermolecular metal scrambling.

Thus, it has been proven that the mixed-metal triangular trimetal sandwich complexes are synthesizable in a selective manner. The present results expand the scope of the structural variability of multinuclear sandwich complexes from homonuclear to heteronuclear series.

3. Reaction Mechanism of Highly Reactive Pd–Pd Complexes

Our group has shown that a homoleptic dinuclear Pd–Pd complexes of nitriles such as $[Pd_2(CH_3CN)_6][BF_4]_2$ are isolable.[5] These homoleptic solvento-Pd_2 complexes are highly substitutionally labile, and allow us to investigate reaction mechanism of the Pd–Pd complexes in details. For example, our group has shown that a Pd–Pd moiety adds to various unsaturated hydrocarbons in a syn addition manner.

Dinuclear Addition of a Pd–Pd Moiety to Arenes[6]

We found that a Pd–Pd moiety undergoes addition reaction to arenes to afford the bi-π-allyl type dipalladium complexes. Previously simple $\mu–\eta^2:\eta^2–$(arene)–Pd_2 complexes have been isolated, but now we found that a Pd–Pd moiety undergoes dinuclear addition to several arenes to afford a novel binding mode of arene–Pd_2, namely $\mu-\eta^3:\eta^3–$(arene)–Pd^{II}_2 (Figure 3), through isolation and characterization of **8'**, **9**, and **10**. The fact that bi-η^3-allyl type structure is accessible via dinuclear syn-addition of a Pd–Pd moiety suggest possible involvement of a new activation mode of arenes by a Pd–Pd species in some palladium-catalyzed transformations.
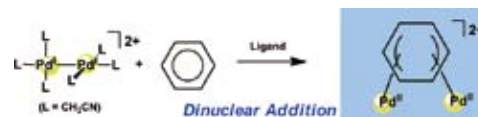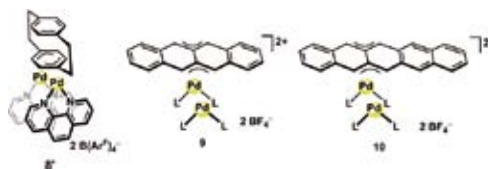

Figure 3. Dinuclear addition of a Pd–Pd moiety to arenes.

References

1) For the first report on the metal chain sandwich complexes: T. Murahashi, *et al.*, *J. Am. Chem. Soc.* **121**, 10660–10661 (1999).

2) For the first report on the metal sheet sandwich complexes: T. Murahashi, *et al.*, *Science* **313**, 1104–1107 (2006).

3) T. Murahashi, K. Shirato, A. Fukushima, K. Takase, T. Suenobu, S. Fukuzumi, S. Ogoshi and H. Kurosawa, *Nat. Chem.* **4**, 52–58 (2012).

4) T. Murahashi, K. Usui, Y. Tachibana, S. Kimura and S. Ogoshi, *Chem. –Eur. J.* **18**, 8886–8890 (2012).

5) T. Murahashi, *et al.*, *J. Am. Chem. Soc.* **128**, 4377–4388 (2006).

6) T. Murahashi, K. Takase, M. Oka and S. Ogoshi, *J. Am. Chem. Soc.* **133**, 14908–14911 (2011).

Development of Functional Metal Complexes for Artificial Photosynthesis

Department of Life and Coordination-Complex Molecular Science
Division of Functional Coordination Chemistry

|	
MASAOKA, Shigeyuki	Associate Professor
KONDO, Mio	Assistant Professor
YOSHIDA, Masaki	Graduate Student*
NAKAMURA, Go	Graduate Student
OKAMURA, Masaya	Graduate Student
MURASE, Masakazu	Graduate Student†
ITOH, Takahiro	Graduate Student
KUGA, Reiko	Technical Fellow
LIU, Ke	Technical Fellow
KANAIKE, Mari	Technical Fellow
WAKABAYASHI, Kaori	Technical Fellow
TANIWAKE, Mayuko	Secretary

Artificial photosynthesis is a solar energy conversion technology that mimics natural photosynthesis, and poised to be one of the next big breakthroughs in energy. Our group studies chemistry of transition metal complexes for the realization of artificial photosynthesis. Efforts have focused on development of new catalysts for multi-electron transfer reactions and understanding the reaction mechanism. During the last year, we reported (i) a mononuclear ruthenium complex showing multiple proton-coupled electron transfer toward multi-electron transfer reactions,[1] (ii) kinetics and DFT studies on water oxidation catalyzed by a mononuclear ruthenium complex,[2] and (iii) two-step photoexcitation of a platinum complex to produce hydrogen from water.[3] We also demonstrated (iv) the self-assembly of microstructures from dinuclear ruthenium complexes and their structural transformation.[4] The research projects (i), (ii) and (iv) are introduced in this report.

1. A Mononuclear Ruthenium Complex Showing Multiple Proton-Coupled Electron Transfer toward Multi-Electron Transfer Reactions[1]

Proton-coupled electron transfer (PCET) is an important chemical process that involves the concerted transfer of a proton (H^+) and an electron (e^-). It is widely employed to achieve multi-electron transfer reactions such as water oxidation by photosystem II and nitrogen fixation by nitrogenase as well as solar energy conversion in artificial photosynthesis, since high-energy intermediates and/or electrostatic charge buildup during the reactions are generally avoided by going through PCET processes.

In this context, we synthesized and characterized a new ruthenium(II) complex, $[Ru(trpy)(H_2bim)(OH_2)](PF_6)_2$ (**1**)

(H_2bim = 2,2'-biimidazole and trpy = 2,2':6',2"-terpyridine), where the H_2bim and $M-OH_2$ moieties in the molecule are expected to serve as proton-dissociation sites. Electrochemical studies in aqueous solutions under various pH conditions afforded the Pourbaix diagram (potential versus pH diagram) of **1**, where the pK_a values found from the diagram agree well with those determined spectrophotometrically. It was also found that **1** demonstrates four-step PCET reactions to give the four-electron oxidized species, $[Ru^{IV}(trpy)(bim)(O)]^{2+}$, without electrostatic charge buildup during the reactions (Figure 1). The multiple PCET ability of **1** would be applicable to various multi-electron oxidation reactions. Catalysis of electrochemical water oxidation was indeed evaluated in the initial attempt to demonstrate multi-electron oxidation reactions, revealing that the water oxidation potential for **1** is lower than that for 2,2'-bipyridine analogue, $[Ru(trpy)(bpy)(OH_2)]^{2+}$ (**2**) (bpy = 2,2'-bipyridine), which is known as an active catalyst for water oxidation.
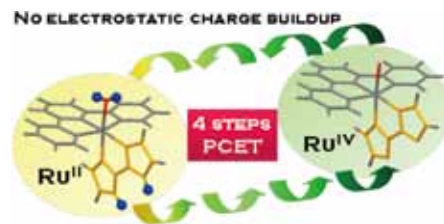
Figure 1. A schematic view of the four-step PCET reaction of **1** to give the four-electron oxidized species, $[Ru^{IV}(trpy)(bim)(O)]^{2+}$.

2. Kinetics and DFT Studies on the Mechanism of Water Oxidation Catalyzed by Mononuclear Ruthenium Complexes[2]

Visible light-induced water splitting is one promising

approach for artificial photosynthesis. This solar-to-fuels conversion consists of the two half-cell reactions; reduction of water to H_2 ($2H^+ + 2e^- \rightarrow H_2$) and oxidation of water to O_2 ($2H_2O \rightarrow O_2 + 4H^+ + 4e^-$). Particularly, development of molecular catalysts for O_2 evolution has been considered more difficult than the hydrogen side, since the O_2 evolution requires removal of four protons and four electrons.

We previously provided two important aspects with regard to this issue as follows. (i) Mononuclear ruthenium catalysts can be classified into two groups based on the rate law observed. One obeys $d[O_2]/dt = k[\text{catalyst}][Ce^{4+}]$ and the other obeys $d[O_2]/dt = k[\text{catalyst}]^2$, where the rate is first- and second-order to the catalyst concentration, respectively. (ii) A radical coupling of the oxo atom from Ru catalyst and the radical-like O(hydroxo) atom from hydroxocerium(IV) species plays an important role in the O–O bond formation in the former monoruthenium-catalyzed O_2 evolution reactions. However, our previous studies has not provided the spectroscopic evidence of the highest-valence intermediate for the Ru species prior to the O–O bond formation.

In this work, the reaction mechanism of the Ce^{4+}–driven water oxidation catalyzed by $[Ru(trpy)(bpy)(OH_2)]^{2+}$ (**2**, Ru^{II}-OH_2). As a result, the Ru^V=O species, together with other intermediates in the multi-step electron transfer processes, were spectrophotometrically followed by use of the global kinetic analysis using the singular value decomposition (SVD) method. We also demonstrate that each spectral component can be rationally reproduced by TD-DFT (time-dependent density functional theory) calculation. Moreover, it is also found that the Ru^V=O species can be written as the resonance structure of the Ru^{IV}-$O^\bullet$ species (Ru^V=O $\leftrightarrow$ Ru^{IV}-$O^\bullet$), indicating that the Ru^V=O species bears a substantial radical character at the O(oxo) atom. This study suggests that a radical-radical coupling of Ru^V=O and hydroxocerium(IV) species predominates the major path leading to the dioxygen formation.
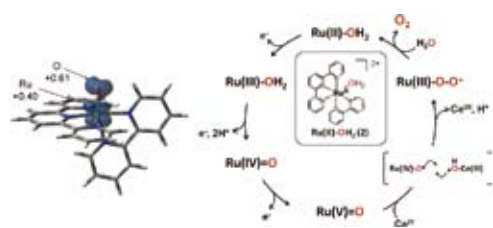
Figure 2. (Left) The optimized structure of the Ru^V=O species in the doublet state. The distribution of the Mulliken atomic spin density is also overlaid. The spin density is located on the 3d orbital of the ruthenium ion (+0.40) and the 2p orbital of the O(oxo) atom (+0.61). (Right) A proposed catalytic cycle of the Ce^{4+}–driven water oxidation catalyzed by **2**.

3. Self-Assembly of Tubular Structures from Dinuclear Ruthenium Complexes and Their Structural Transformation[4)]

Controlled self-assembly of metal complexes is of high scientific and technological importance for the development of multi-functional materials and devices. Among various types of metal complexes, mixed-valence complexes have attracted much attention because of their wide range of interesting physical and chemical properties from charge-transfer interactions between metal ions linked via bridging ligands. In particular, low-dimensional assembly of such mixed-valence complexes gives rise to specific electronic, magnetic, and optical properties. Ideally, the characteristics of such systems would be tunable by controlling the spatial arrangement of the mixed-valence complexes, resulting in electric interaction among metal complexes without linkage of covalent or coordination.

In this work, we have demonstrated that the lipid-packaged mixed-valence complex displays morphological changes with aging of the solution in dichloromethane. Formation of a bilayer structure causes morphological evolution from micro-tapes to microtubes, giving rise to changes in absorption spectral intensities. Moreover, these morphological and spectral changes can be reversed by standing or shaking. The technique of combination of lipid molecules and *discrete* coordination compounds makes it possible to design flexible, reversible and signal responsive supramolecular coordination systems. The concept of lipid packaging could also be expanded of other useful coordination compounds, and should allow us to further develop the nanochemistry of coordination materials.
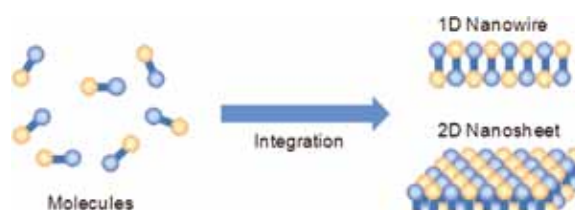
Figure 3. Schematic illustration of the assembly of discrete metal complexes for constructing nanostructures.

References

1) M. Okamura, M. Yoshida, R. Kuga, K. Sakai, M. Kondo and S. Masaoka, *Dalton Trans.*, in press.
2) A. Kimoto, K. Yamauchi, M. Yoshida, S. Masaoka and K. Sakai, *Chem. Commun.* **48**, 239–241 (2012).
3) M. Kobayasi, S. Masaoka and K. Sakai, *Angew. Chem., Int. Ed.* **51**, 7431–7434 (2012).
4) K. Kuroiwa, M. Yoshida, S. Masaoka, K. Kaneko, K. Sakai and N. Kimizuka, *Angew. Chem., Int. Ed.* **51**, 656–659 (2012).

Award
KONDO, Mio; The 5th Shiseido Female Researcher Science Grant (2012).

* carrying out graduate research on Cooperative Education Program of IMS with Kyushu University
† carrying out graduate research on Cooperative Education Program of IMS with Nagoya Institute of Technology

Visiting Professors

Visiting Professor
SASAI, Hiroaki *(from Osaka University)*

Design and Synthesis of Novel Enantioselective Catalysts and Their Application

    Synthesis of optically active complex molecules using catalytic amount of chiral compounds plays an important role in pharmaceutical industrial processes. Our group engages in the development of novel enantioselective catalyses which involve asymmetric domino reaction promoted by an acid-base type organocatalyst, oxidative coupling of 2-naphthol derivatives using dinuclear vanadium(V) catalysts, spiro bis(isoxazoline) ligand (SPRIX) accelerated Pd catalyses, *etc*. Recently we have realized a highly enantioselective intramolecular Rauhut-Currier reactions catalyzed by an amino acid derived organocatalyst. In addition, an umpolung acetoxylation of Pd enolate derived from alkynyl cyclohexadienones was found to be promoted by Pd-SPRIX catalyst.

Visiting Associate Professor
UEMURA, Takashi *(from Kyoto University)*

Polymer Chemistry in Coordination Nanospaces

    One of the most outstanding challenges in polymer materials science is the fabrication of systems that allow the controlled arrangement of monomers to be polymerized to materials useful for a desired purpose. We are developing strategies to control polymerizations in nanochannels of Metal–Organic Frameworks (MOFs) composed of metal ions and organic ligands. Use of their regulated and tunable channels for a field of polymerization can allow multi-level controls of the resulting polymer structures, such as molecular weight, stereoregularity, reaction positions, and monomer sequences. In addition, construction of nanocomposites between MOFs and polymers provides new material platforms to accomplish many optical and electronic functions.

Visiting Associate Professor
SUDO, Yuki *(from Nagoya University)*

Understanding and Controlling the Photoactive Proteins

    Light is one of the most important energy sources and signals providing critical information to biological systems. Rhodopsin molecules are photochemically reactive membrane-embedded proteins, with seven transmembrane α-helices which bind the chromophore retinal (vitamin A aldehyde). A striking characteristic of these photoactive proteins is their wide range of seemingly dissimilar functions. We are investigating them by using various techniques such as biophysical, molecular biological, biochemical, genetical and spectroscopic methods. In addition, rhodopsin molecules have great potential for controlling cellular activity by light. We are also focusing on the development of novel photocontrollable tools for the life scientists.